Karstification below dam sites: a model of increasing leakage from reservoirs

W. Dreybrodt · D. Romanov · F. Gabrovsek

Abstract Unnaturally steep hydraulic gradients below foundations or across abutments of dams may cause solutional widening of fractures in karstifiable rocks of carbonates or gypsum. This could cause increasing leakage which may endanger the performance of the construction. To investigate this problem recent models on natural karstification have been applied. We have performed numerical simulations of leakage below a model dam with a grouting curtain reaching down to 100 m below its impermeable foundation of 100 m width. Water is impounded to a depth of 100 m. The dam is located on a terrane of fractured rock dissected by two perpendicular sets of fractures with spacing of 5 m, and with a log-normal distribution of their initial aperture widths of about 0.02 cm. In the first state of karstification these fractures widen slowly, until a pathway of widened fractures below the grouting has reached the downstream side with exit widths of about 1 mm. This causes a dramatic increase of leakage, and turbulent flow sets in. After this breakthrough at time T, in the second state of karstification, dissolution rates become even along these fractures and cause widening of about 0.1 cm year^{-1} for limestone, and at least of 1 cm year^{-1} for gypsum. This leads to an increase in leakage to excessive rates within 25 years for limestone, but only 5 years for gypsum. We have performed a sensitivity analysis of breakthrough time T for the various parameters which determine the problem. The result shows breakthrough times in the order of several tens of years for both limestone and gypsum. We have also modelled leakage to caves or karst channels 200 m below the bottom of the reservoir, which could induce the formation of sinkholes. The model can be extended to more realistic settings. In conclusion, our results support the prediction that increasing leakage at dam sites can be caused by recent karstification which is activated after filling the reservoir, possibly leading to serious problems within its lifetime.

Keywords Dam site · Karstification · Leakage · Limestone · Gypsum

Received: 17 September 2001 / Accepted: 16 October 2001
Published online: 15 February 2002

W. Dreybrodt (✉) · D. Romanov
Karst Processes Research Group, Institute of Experimental Physics, University of Bremen, 28334 Bremen, Germany
E-mail: dreybrod@physik.uni-bremen.de
Tel.: +49-421-2183556
Fax: +49-421-2187318

F. Gabrovsek (✉)
Karst Research Institute, Postojna, Slovenia
E-mail: gabrovsek@zrc-sazu.si

Introduction

Due to their hydrogeological complexity, karst terranes have been considered problematic as sites for the construction of large hydroprojects, including dams and reservoirs. Nevertheless, owing to the increasing demand for water, and the fact that more than 20% of the earth's surface is underlain by soluble rocks, a large number of dams have been constructed successfully world wide. The present state of the art in constructing large dams has benefited from many failures in the past. For example, some reservoirs could not retain water and others could even never be filled. Some reservoirs suffered from increasing water loss resulting from gradual opening of joints and channels filled with sediments. A list of leakages from 42 dams world wide is given by Milanovic (2000). Filling of a reservoir causes a first immediate impact to the environment. It also causes a change of the boundary conditions to the karst aquifer. Unnaturally large hydraulic gradients are created and new pathways of flow, even initially with negligibly small flow rates, may be activated. These new conditions change the pattern of karstification, which is a highly dynamic process, and is likely to be accelerated under the extremely high hydraulic gradients. Consequently, even if water loss is low after first filling of the reservoir, it may increase in time. The Great Falls Reservoir, USA showed an increase of leakage from 0.47 m^{3}s^{-1} in 1926 to 6.6 m^{3}s^{-1} in 1939, and to 12.7 m^{3}s^{-1} in 1945, which caused a decrease of its water level by 8.1 m (Milanovic 2000).

 DOI 10.1007/s00254-001-0514-7

Thus, the possibility arises that enhanced karstification could lead to increasing leakage by creating new karst channels below the grouting and across the abutments of the dam. This slow environmental change may not be perceived in its early stage of evolution, but may subsequently lead to severe environmental impacts on the integrated system of natural karst aquifer–hydraulic structure.

To understand the processes of the early state of conduit evolution in karstifying limestone, one- and two-dimensional models have been developed which couple flow rates of calcite aggressive water to dissolutional widening of initially narrow fractures (Dreybrodt 1990; Palmer 1991; Groves and Howard 1994; Dreybrodt 1996; Siemers and Dreybrodt 1998; Palmer 2000; Dreybrodt and Gabrovsek 2000; Dreybrodt and Siemers 2000). These models reveal a positive feedback loop coupling the rate of dissolutional widening to the flow rate of the aggressive water, driven by a constant head from an input of a percolating pathway of fractures to its output. This positive feedback loop causes an initially slow increase of the fracture widths and the flow rates, which is suddenly enhanced dramatically. The time when this happens is termed the breakthrough time T. From then on, constant head conditions of flow break down because, under most natural conditions, such high flow rates can no longer be supported by the limited amount of water available at the input.

The cause for the breakthrough behaviour is the nonlinear dissolution kinetics of limestone (Eisenlohr and others 1999; Dreybrodt and Eisenlohr 2000), by which the dissolution rates are given as

$$F_1(c) = k_1(1 - c/c_{eq}) \;\; for \;\; c \le c_s$$
$$F_n(c) = k_n(1 - c/c_{eq})^n \;\; for \;\; c > c_s \qquad (1)$$

where c is the concentration of calcium in the calcite aggressive water, c_{eq} is its equilibrium concentration with respect to calcite, $c_s \approx 0.9 c_{eq}$ is the switch concentration where the kinetics switches from a linear rate law to a nonlinear one with order n≈4, k_1, and k_n are rate constants in mol cm^{-2} s^{-1}. Recent research on gypsum rocks has revealed a similar rate law also for this mineral (Jeschke and others 2000).

Using these rate laws in the models enables one to give analytic estimations of T, which reveals the parameters which determine early karstification. These are initial aperture width a_0 of the fracture, the distance L between input and output, the hydraulic head h, and the chemical parameters n, k_n, c_s and c_{eq}. From these parameters the breakthrough time T can be estimated for single fractures (Dreybrodt 1996; Dreybrodt and Gabrovsek 2000), and for percolation networks on a square lattice (Siemers and Dreybrodt 1998; Dreybrodt and Siemers 2000) by

$$T = \left(\frac{1}{a_0}\right)^{\frac{2n+1}{n-1}} \left(\frac{L^2\eta}{hc_{eq}}\right)^{\frac{n}{n-1}} \cdot (k_n)^{\frac{1}{n-1}} \cdot const \qquad (2)$$

where η is the dynamic viscosity of water, and the constant can be estimated for single conduits and simple networks.

After breakthrough the concentration c in the conduits drops close to zero and dissolutional widening is even along the conduit at about 1 mm year^{-1} for limestone (Buhmann and Dreybrodt 1985) and at least 1 cm year^{-1} for gypsum (James 1992; Jeschke and others 2000).

Close to hydraulic structures in karst regions, such as dam sites or artificial underground reservoirs created by plugging karst channels (Milanovic 2000), hydraulic heads are extremely high, and pathways of flow from the reservoir to base level are comparably short. Therefore, extremely steep hydraulic gradients arise. This raises the question whether karstification below dams could be so fast that, within their lifetimes, leakage increases to excessive amounts. First models to answer this question have been developed for one-dimensional conduits by Palmer (1988) and Dreybrodt (1992, 1996). Both authors found comparable results, demonstrating that hydraulic structures may be seriously affected within time spans of 100 years. Such single conduit models, however, are not realistic since no exchange of water between the evolving conduits and the surrounding fractures is considered. If water is allowed to flow from an evolving conduit into the net of fractures, more aggressive input water is driven along it and dissolution rates should be higher. This should accelerate its evolution. First approaches to this have been reported by Bauer and others (1999).

In this work we deal with a two-dimensional cross section of a dam site, where the underlying rock is dissected by two perpendicular sets of fractures with a statistical distribution of their aperture widths. The spacing and the apertures of the fractures are chosen such that the hydraulic conductivity of the limestone is about 10^{-6} m s^{-1}, representative for moderately karstified rock.

Model structure

The model consists of a two-dimensional cross section of the soluble rock below the dam (see Fig. 1). The modelling

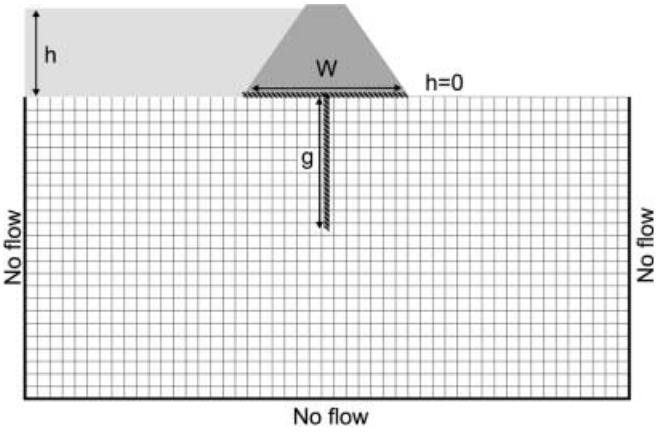

Fig. 1
The model dam with fractured rocks below. Water is impounded to the *left*. The impermeable base and the grouting curtain are also shown

domain is 500 m wide and 250 m deep. The fractures are represented by a square net with a spacing of 5×5 m. This creates a network of 100×50 squares. The width of all fractures is 1 m. To account for the heterogeneity of the fracture system, we assign a selected aperture width to each fracture within the net. Furthermore, it is possible to consider different lithologies of the bedrock by assigning to each fracture different values of the dissolution rate constants k_1, n, k_n and c_{eq}. In this way, one is able to model also regions of insoluble rock or of highly soluble gypsum, located in the model domain. The impermeable dam with width W at its basis is also shown in Fig. 1. At its left-hand side water is impounded to depth h, supplying a constant head boundary condition. At its right-hand side, downstream, the hydraulic head is constant at zero. An impermeable grouting curtain below the dam extends to depth g. The lower domain boundary as well as the left-hand and right-hand borders are assumed as impermeable. Water flow in the net is assumed to be laminar. The calculation of the head h_t for node i is based on mass conservation for each node, i.e. flow rate into the node is equal to that leaving it. The resistance of each fracture is calculated by the Hagen-Poiseuille law. The resulting set of linear equations is solved by the preconditioned conjugate gradient method for sparse matrices (Steward and Leyk 1994). Once all heads are known, the flow rate in each fracture is calculated. Dissolutional widening F in each fracture is then calculated from the flow rates and the rate law of dissolution (Eq. 1). Details are given by Siemers and Dreybrodt (1998), and Gabrovsek (2000). To obtain the aperture-width profiles of the fractures and the flow rates as a function of time, we use an iterative procedure. If $a(x,t)$ is the profile of fracture i along the co-ordinate x after a sufficiently short time step Δt, the new width profile is given by

$$a(x, t + \Delta t) = a(x, t) + 2\gamma F(x, t) \cdot \Delta t \qquad (3)$$

where $\gamma F(x,t)$ is the retreat of bedrock in cm year^{-1}, and Δt is a time step in years. After each time step, laminar flow in all fractures is assured by calculating the Reynolds Number Re which remains well below 2,000 until breakthrough occurs. The run is terminated when Re exceeds 2,000.

The model dam on limestone

Figure 2a–c show a scenario which is typical for a dam in limestone. The results for a dam in gypsum are also illustrated, but will be discussed below. The width of the dam is 100 m, grouting depth g=100 m, and the depth h of the impounded water is 100 m. The fracture net consists of fractures 1 m wide, with a log-normal statistical distribution of their initial aperture widths with mean a_0=0.02 cm and $\sigma \approx 0.01$ cm. The chemical parameters have been taken as $k_1 = 4 \cdot 10^{-11}$ mol cm^{-2} s^{-1}, $k_4 = 4 \cdot 10^{-8}$ mol cm^{-2} s^{-1}, $c_{eq} = 2 \cdot 10^{-6}$ mol cm^{-3}, c_s=0.9 c_{eq}. These are typical for limestone (Dreybrodt and Eisenlohr

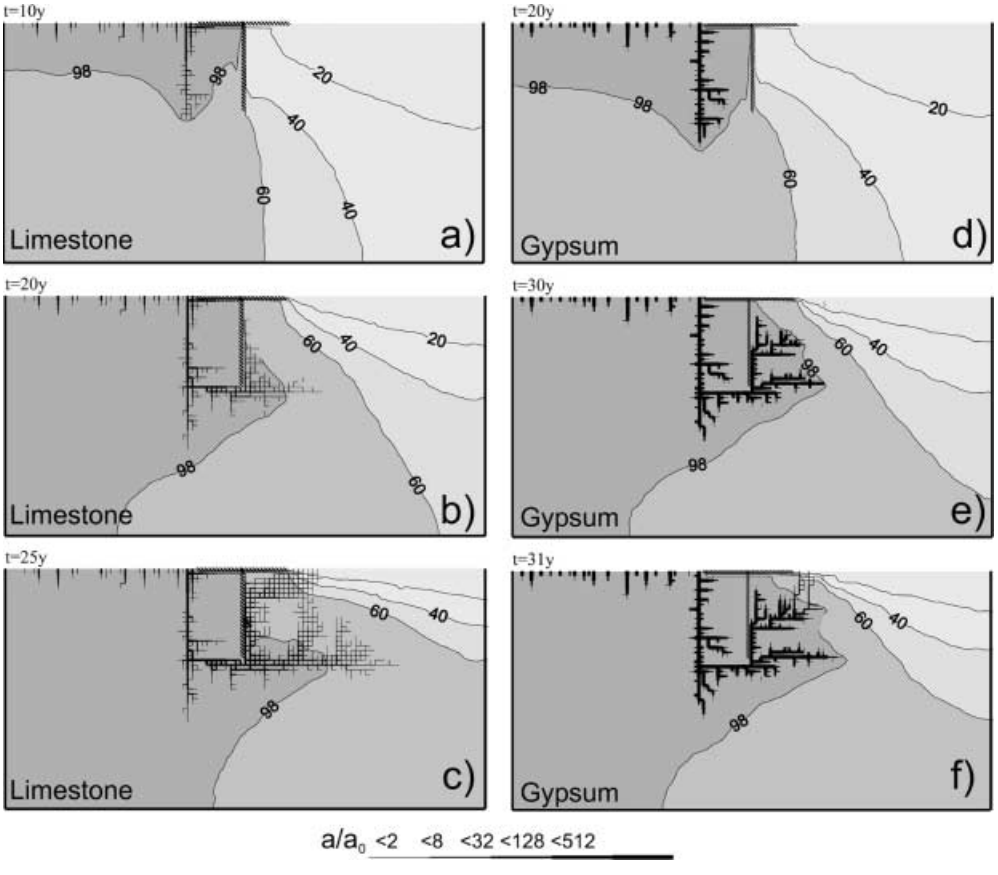

Fig. 2e–f
Evolution of karst channels below the model dam after filling the reservoir. **a–c** Limestone after 10, 20 and 25 years respectively. Breakthrough occurs at 25 years, when the fractures at the exit have widened to about 0.1 cm. **d–f** Evolution in gypsum for comparison at 20, 30 and 35 years respectively. The *bars* at the bottom indicate the widths of the fractures in multiples of the initial aperture width a_0

2000). In this scenario we assume allogenic water with low calcium concentration impounded in the reservoir. Therefore, the concentration of the water entering the fractures has been taken as c_0=0.
Figure 2a shows the situation 10 years after filling the reservoir. First small channels start to grow. Close to the horizontal impermeabilisation, a main channel has penetrated downwards to about 100 m. The pressure isolines are also shown, to illustrate the distribution of hydraulic gradients. These are steepest just below the grouting curtain. Therefore, flow is concentrated into this region. Consequently, dissolutional widening is most active here and, after only 20 years, a net of small channels with widths of about 1 mm has grown below the grouting. The steepest hydraulic gradient is now close to the right-hand side of the grouting wall, and widening creates a channel directed upwards (Fig. 2b). After further 5 years, this channel has reached the surface, and other channels follow the steep hydraulic gradients upwards (Fig. 2c). The fracture widths at these exits are about 0.1 cm. Figure 3 shows the evolution of leakage Q in time. Three phases of behaviour can be observed:

1. A small increase in Q during the first 15 years.
2. After this time, channels have approached closer to the surface and the total resistance to flow has decreased because only the region of steep gradients is utilised for flow. Therefore, as the channels approach closer to the surface, total flow increases.
3. Finally, when the first channel has reached the surface, breakthrough occurs and flow increases steeply. The run was terminated when turbulence sets in at a total leakage of 2,000 $cm^3\ s^{-1}$. For a dam with a width of 100 m, this amounts to a leakage of 0.2 $m^3\ s^{-1}$. Shortly after breakthrough, the calcium concentration becomes less than 0.1 c_{eq} everywhere in the leading flow path, and dissolution rates are high and even, causing fracture widening of about 1 mm $year^{-1}$ (Buhmann and Dreybrod 1985). This will not change during turbulent flow.

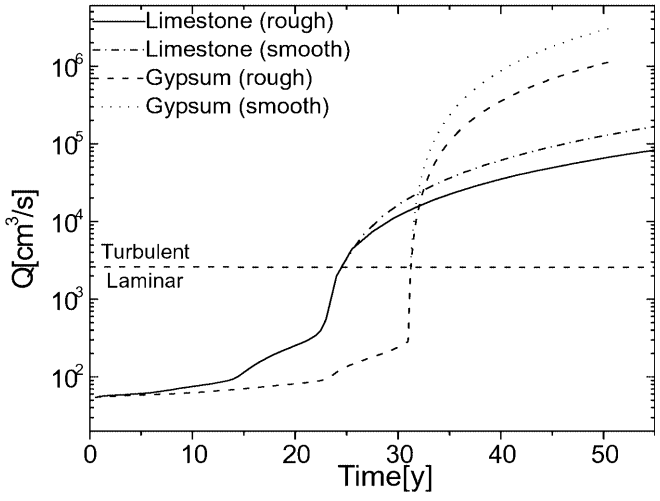

Fig. 3
Evolution of leakage Q below the dam for limestone (*closed line*) and gypsum (*dotted line*). The units of Q refer to the model section with 1-m widths of the fractures. The total leakage is found by multiplying with the width of the dam in metres. The lower part of the plot depicts the phase with laminar flow. At breakthrough turbulent flow sets in. The evolution of turbulent flow has been estimated for smooth and rough channels (see text). The limit of unbearable water loss is at $10^5\ cm^3\ s^{-1}$, which corresponds to about 10 $m^3\ s^{-1}$ for a dam with a width of 100 m

The further evolution of leakage can be estimated to a lower limit in the following way. The flow path of about 300 m length is approximated by one single straight channel with the hydraulic diameter of its exit, everywhere along the channel. For such a single channel, we use the Darcy-Weisbach equation and the Colebrook-White formula for the friction coefficient to calculate the flow as a function of the fracture width of the channel (Dreybrodt 1988). This estimation is also depicted in Fig. 3. Two limits are given. The upper curve is for a completely smooth channel, whereas the lower represents flow in a rough channel with a roughness of 10% of the channel width. The flow rates increase in time t by a power law $Q \propto t^{3/2}$. About 25 years after breakthrough, they have increased to about 100 l s^{-1} per metre of dam. For a dam 100 m wide, this amounts to 10 $m^3\ s^{-1}$. One should keep in mind that this is a lower limit. We will extend our programme to turbulent flow to get more detailed information.

The model dam in gypsum

In this scenario we change the underlying rock from limestone to gypsum. This is achieved by changing the constants of dissolution to those of gypsum. These are (Jeschke and others 2000) $k_1=1.3\cdot10^{-7}$ mol $cm^{-2}\ s^{-1}$, $k_n=3\cdot10^{-3}$ mol $cm^{-2}\ s^{-1}$, n=4.5, and $c_{eq}=15.4\cdot10^{-6}$ mol cm^{-3}.
In all computer runs and in the same way as for limestone, we have calculated the rates for pure diffusion control and compared them to the surface-controlled rates. Then, the smaller rates were used. Figure 2d–f shows the results for the channel patterns after 20 and 30 years, and at breakthrough one year later. The behaviour is similar to that of Fig. 2a–c although, owing to the much higher dissolution rates, all channels are significantly wider. At breakthrough the exit widths are about 2 mm. The evolution of the flow rates is shown in Fig. 3. After breakthrough calcium concentrations are less than 0.1 c_{eq}. Dissolution rates are therefore high, at least 10 mm $year^{-1}$ (James 1992). Although with increasing flow rates the dissolutional widening may rise up to 10 cm $year^{-1}$, we use the lower values to give a lower limit estimation. Figure 3 shows also this estimation for turbulent flow. Only 5 years after breakthrough, leakage rates have increased to 100 l s^{-1}.
In this context, the main difference between limestone and gypsum is not the evolution of pathways before breakthrough. These are similar. It is the huge difference in the dissolution rates after breakthrough, which causes the much faster increase of leakage at gypsum sites. Although this gypsum scenario might not be very realistic, it has

been described here for didactic reasons. More realistic scenarios, where gypsum occurs as layers in strata of clays, limestone, or sandstone can be handled by our model. This will be the target of further work.

Sensitivity analysis

To gain some estimation on the dependence of breakthrough times on the various parameters, we used our model scenarios on limestone and on gypsum, and have varied one parameter, leaving all the others unchanged. However, in doing so, we have used different realisations of the statistical distribution of aperture widths. If one uses several different realisations, leaving everything else unchanged, breakthrough times vary by about ±15%. This has been taken for the error bars in Fig. 4. Figure 4a depicts the dependence of breakthrough times on the average aperture widths a_0 of the fractures. Breakthrough times increase steeply with decreasing aperture width. They follow roughly a power law $T \propto a_0^{-3.8\pm0.2}$ which is close to the behaviour of breakthrough times for single conduits (cf. Eq. 2). Figure 4b depicts the dependence of T on the head, h, which can be approximated by $T \propto h^{-1.3\pm0.3}$. With increasing depth g of grouting, breakthrough times increase significantly for grouting depths larger than the impounded height h of the water (see Fig. 4c). An important parameter for dissolutional widening is the chemical composition of the water at the bottom of the lake, which determines both the input concentration c_0 to the fractures, and c_{eq} for limestone. Figure 4d depicts the dependence of T on c_0. There is only little change for $c_0 < 0.5 c_{eq}$. If the water becomes more saturated, however, breakthrough times increase. After breakthrough the concentration drops to c_0 along the leading fractures, and dissolution rates are accordingly lower. Thus, the chemistry at the bottom of the lake is of utmost importance for limestone. In the case of gypsum, however, c_{eq} does not depend on the CO_2 concentration in the lake. Moreover, impounded waters are usually not close to saturation with respect to gypsum. Therefore, c_0 is much smaller than c_{eq}. Finally, in Fig. 4e we show the influence of c_{eq} on T for limestone, which again recalls single channel behaviour with $T \propto c_{eq}^{-1.3\pm0.2}$. The boundary conditions of the impermeable right- and left-hand sides of the domain may appear unrealistic since the soluble rocks may extend much further. We have therefore changed the domain width to

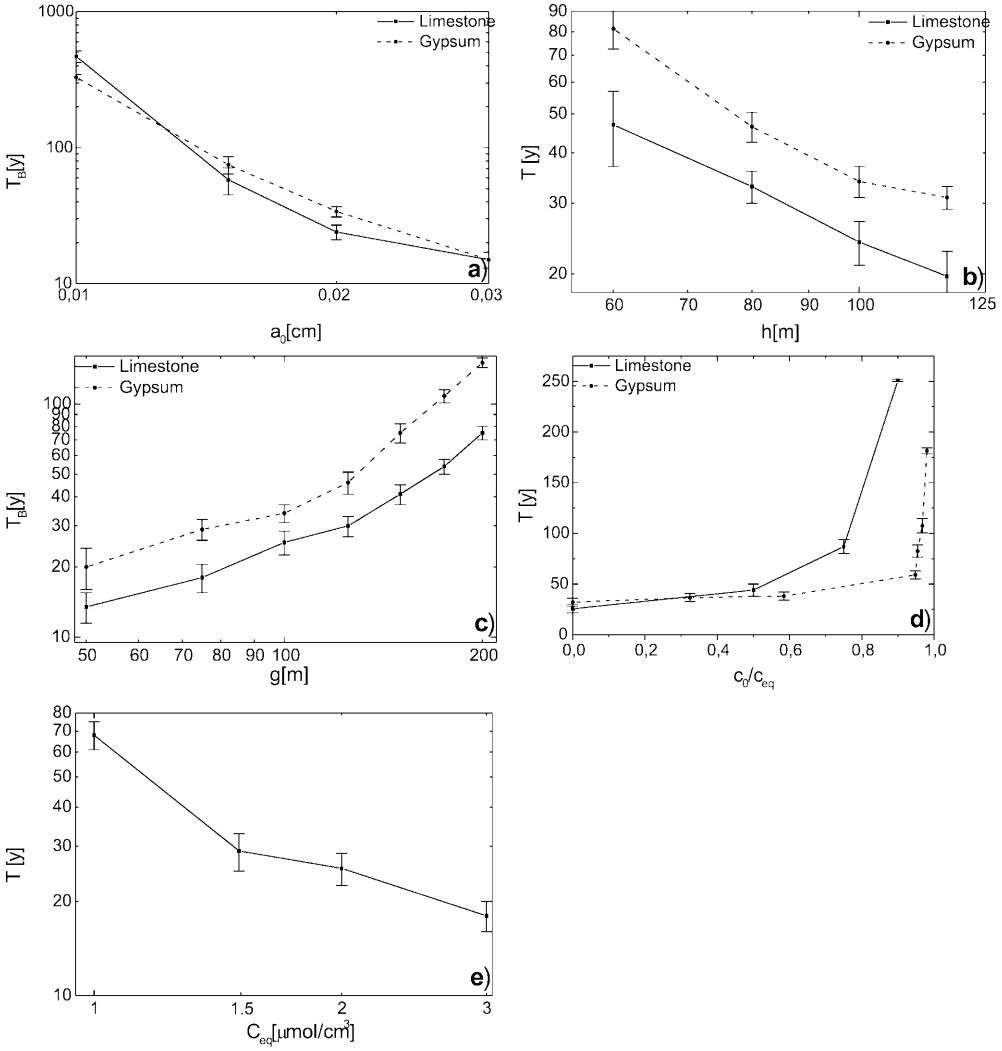

Fig. 4a–e
Dependence of breakthrough time T on **a** the initial aperture width of the fractures, **b** the height of impounded water, **c** the depth of grouting, and **d** the saturation state of the lake water for both limestone (*closed lines*) and gypsum (*dotted lines*). In all gypsum data c_{eq}=15.4 mmol cm^{-3}. **e** Dependence of T on c_{eq} for limestone

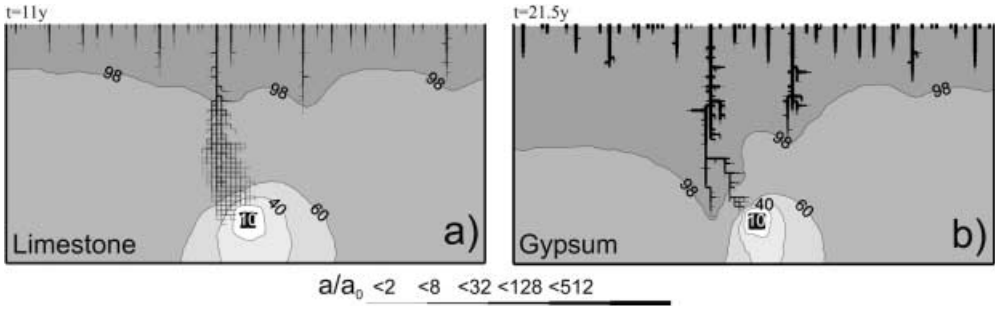

Fig. 5a, b
First stage of sinkhole evolution at breakthrough in **a** limestone, and **b** gypsum. The *shaded square* represents a karst channel at hydraulic head of 10 m, located 200 m below the reservoir bottom. Depth of the impounded lake is 100 m. The isolines of the head show the head contribution and illustrate the hydraulic gradient. The *bars* at the bottom indicate fracture widths in multiples of initial fracture width a_0

1,000 m, using a 200 by 50 net. No changes in breakthrough times were found.

Sinkholes

For a conference on sinkholes it is mandatory to deal with them also in this context. The formation of sinkholes on the floors of water reservoirs in karstic areas is a well-known problem. If caves or karst conduits are located deep below the bottom of a lake, a pathway of dissolutional widening could be directed from the floor of the reservoir to these conduits. We have assumed that such conduits are located 200 m below. The location of the cave is marked by a shaded square in Fig. 5. In the model we assign a hydraulic head of 10 m to all nodes comprising this area. Thus, we simulate a large conduit completely filled with water which is directed towards a spring with an elevation of 10 m. In the case of a vadose cave, the head which should be chosen would be h=–200 m, the depth of location below ground. The network of fractures has been created with the standard log-normal distribution of aperture widths, with the same distribution as in the cases above. Figure 5a shows the result at breakthrough for a limestone terrane. For limestone, breakthrough is reached after only 11 years and the fractures at the cave have been widened to about 0.1 cm. After breakthrough, subsequent evolution of leakage through this region is determined by turbulent flow and can be estimated by assuming a straight channel downwards as has been described above. Figure 5b shows what happens when limestone is replaced by gypsum, everything else having been left unchanged. Due to the different dissolution kinetics, breakthrough is achieved after 21 years, at which time aperture widths close to the cave are about 0.2 cm. Such nets of small channels, as shown in Fig. 5, can be regarded as initial states of sinkholes. To find out how they develop requires extension of the programme to turbulent flow, a phase which currently is in progress.

Conclusion and further perspectives

We have presented a computer model of karstification below dam sites and demonstrated that leakage from these hydraulic structures can be caused by dissolutional widening of initially narrow fractures of about 0.02 cm aperture widths. Such a geological situation, with such narrow fractures present solely, is highly idealised. This is also seen from the initial leakage rates (cf. Fig. 3). For our standard dam with a width of 100 m, initial leakage is only 6 l s^{-1}, which would be ideal for each dam. In reality, even in moderately karstified regions there will be wider fractures and small channels distributed underground. This will greatly reduce breakthrough times. To obtain an idea about this, we have assigned aperture widths of 0.035 cm to 30% of the fractures in our statistical standard. This was done by selecting each fracture and replacing its width by 0.035 cm with an occupation probability of 0.3. Such a percolation net will not show percolating pathways connecting inputs and outputs by these wide fractures solely

Fig. 6a, b
Conduit pattern and breakthrough for the scenarios of Fig. 2 in **a** limestone and **b** gypsum, but 30% of the fractions have a width of 0.035 cm. These fractures are evenly distributed on the entire net. A section is shown for illustration on the lower *left-hand side* of the net. In contrast to Fig. 2, maze-like patterns are generated

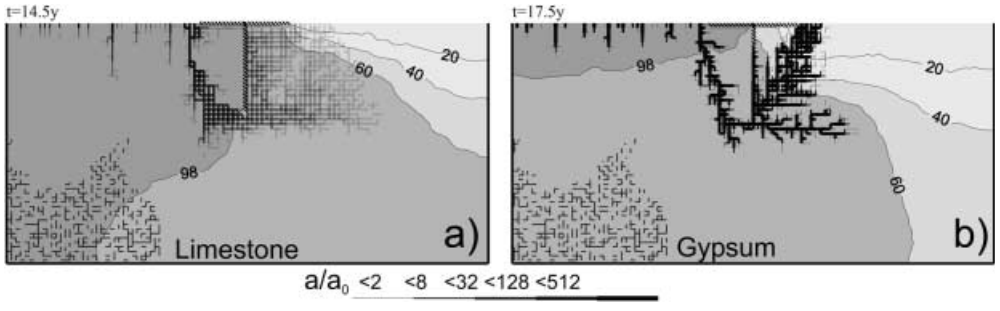

(Siemers and Dreybrodt 1998). Breakthrough times are reduced to half of those of the corresponding standard case. The conduit evolution at breakthrough is illustrated by Fig. 6. Although the changes in aperture widths seem to be moderate, there is a striking difference of the conduit patterns compared to Fig. 2. The more dentitic pattern here is now replaced by a maze, with many more fractures contributing to the leakage from the reservoir. This shows that details in the structure of the rock below the dam site are of high relevance. Realistic geological settings require to incorporate into the programme wider fractures, fault zones, and already existing karst channels. This needs an intensive exchange of information between modellers and civil engineers. To extend the programme to such highly complex situations is tedious but should not present major problems. In this paper we have attempted to show, for relatively simple cases, that karstification below dam sites and close to other hydraulic structures may be induced by unnaturally steep hydraulic gradients acting along unnaturally short pathways of a few hundred metres. Although these models cannot claim that their predictions are highly reliable, they give hints to what may occur during the lifetime of the dam, but probably after the lifespan of those who built it.

References

Bauer S, Birk S, Liedl R, Sauter M (1999) Solutionally enhanced leakage rates of dams in karst regions. In: Palmer AN, Palmer MV, Sasowsky ID (eds) Karst modeling. Karst Waters Institute Inc, Charles Town, West Virginia, Spec Publ 5

Buhmann D, Dreybrodt W (1985) The kinetics of calcite dissolution and precipitation in geologically relevant situations of karst areas: 2. closed system. Chem Geol 53:109–124

Dreybrodt W (1988) Processes in karst systems – physics, chemistry and geology. Springer Series in Physical Environments 4. Springer, Berlin Heidelberg New York

Dreybrodt W (1990) The role of dissolution kinetics in the development of karstification in limestone: a model simulation of karst evolution. J Geol 98:639–655

Dreybrodt W (1992) Dynamics of karstification: a model applied to hydraulic structures in karst terranes. Appl Hydrogeol 1:20–32

Dreybrodt W (1996) Principles of early development of karst conduits under natural and man-made conditions revealed by mathematical analysis of numerical models. Water Resour Res 32:2923–2935

Dreybrodt W, Eisenlohr L (2000) Limestone dissolution rates in karst environments. In: Klimchouk A, Ford DC, Palmer AN, Dreybrodt W (eds) Speleogenesis: evolution of karst aquifers. Natl Speleol Soc USA, pp 136–148

Dreybrodt W, Gabrovsek F (2000) Dynamics of the evolution of a single karst conduit. In: Klimchouk A, Ford DC, Palmer AN, Dreybrodt W (eds) Speleogenesis: evolution of karst aquifers. Natl Speleol Soc USA, pp 184–193

Dreybrodt W, Siemers J (2000) Cave evolution on two-dimensional networks of primary fractures in limestone. In: Klimchouk A, Ford DC, Palmer AN, Dreybrodt W (eds) Speleogenesis: evolution of karst aquifers. Natl Speleol Soc USA, pp 201–211

Eisenlohr L, Meteva K, Gabrovsek F, Dreybrodt W (1999) The inhibiting action of intrinsic impurities in natural calcium carbonate minerals to their dissolution kinetics in aqueous H_2O–CO_2 solutions. Geochim Cosmochim Acta 63:989–1002

Gabrovsek F (2000) Evolution of early karst aquifers: from simple principles to complex models. Zalozba ZRC, Ljubljana, Slovenia

Groves CG, Howard AD (1994) Early development of karst systems. 1. Preferential flow path enlargement under laminar flow. Water Resour Res 30:2837–2846

James AN (1992) Soluble materials in civil engineering. Ellis Horwood Series in Civil Engineering. Ellis Horwood, Chichester

Jeschke AA, Vosbeck K, Dreybrodt W (2000) Surface controlled dissolution rates in aqueous solutions exhibit nonlinear dissolution kinetics. Geochim Cosmochim Acta 65:13–20

Milanovic PT (2000) Geological engineering in karst. Zebra, Belgrade

Palmer AN (1988) Solutional enlargement of openings in the vicinity of hydraulic structures in karst regions: In: Proc 2nd Conf Environmental Problems in Karst Terranes and Their Solutions. Assoc Groundwater Sci Eng Proc, pp 3–15

Palmer AN (1991) The origin and morphology of limestone caves. Geol Soc Am Bull 103:1–21

Palmer AN (2000) Digital modeling of individual solution conduits. In: Klimchouk A, Ford DC, Palmer AN, Dreybrodt W (eds) Speleogenesis: evolution of karst aquifers. Natl Speleol Soc USA, pp 194–200

Siemers J, Dreybrodt W (1998) Early development of karst aquifers on percolation networks of fractures in limestone. Water Resour Res 34:409–419

Steward DE, Leyk Z (1994) Meschach: the matrix computation in C. Australian National University, Canberra, Proc Centre Math Appl 32